IIETA International Information and Engineering Technology Association
Advancing the World of Information and Engineering

Annales de Chimie - Science des Matériaux
Vol. 50, No. 1, February, 2026, pp. 1-11
Journal homepage: http://iieta.org/journals/acsm

Oxide Effect on the Dielectric Behavior of a Ternary Titanate-Based Composite: Exploration on Broadband Dielectric Permittivity

Daoud Kouzrit[1*], Habib Khouni[1], Nacerdine Bourouba[1], Nacerdine Bouzit[1], Abdelhalim Brahimi[1,2], Martinez J. Juan Pablo[3]

[1] Laboratoire d'Instrumentation Scientifique LIS, Electronics Department, Faculty of Technology, University Setif 1 - Ferhat Abbas, Setif 19000, Algeria
[2] ETA Laboratory, Department of Electronics, IET Institute, University Mohamed El Bachir El Ibrahimi of Bordj Bou Arréridj, Bordj Bou Arréridj 34000, Algeria
[3] Departamento de Física Aplicada, Faculty of Science, Zaragoza University, Zaragoza 50009, Spain

Corresponding Author Email: daoud.kezrit@univ-setif.dz

https://doi.org/10.18280/acsm.500101

Received: 12 December 2025
Revised: 11 February 2026
Accepted: 19 February 2026
Available online: 28 February 2026

Keywords:
composite, dielectric materials, modeling, mixture law, permittivity, ternary composite

ABSTRACT

This article examines the dispersion phenomenon and the influence of silicon dioxide (SiO_2) on the complex permittivity of binary composites made of epoxy resin (RE) and barium titanate ($BaTiO_3$). Using Time-Domain Spectroscopy (TDS), the samples were characterized over a frequency range from DC to 30 GHz. The volume fraction-dependent relative permittivity of these composites was modeled using the modified Lichtenecker mixing law (MLL). Numerical optimization was employed to refine the model parameters, offering predictive insights into dielectric permittivity and shape factor coefficients for ternary composites. Comparative analysis confirms the model's suitability for binary and ternary composites, with an efficiency estimated at an average error of less than 2%. A Lorentzian resonance model is proposed to characterize the frequency-dependent behavior of the complex permittivity. The frequency dispersion profile of this ternary composite permittivity, exhibiting both relaxation and resonance spectra, shows a clear evolution with increasing $BaTiO_3$ content. Our empirical model provides a robust description of the resonance-type complex permittivity for $BaTiO_3$ and silica composites. The inclusion of SiO_2 in the binary composite produced remarkable effects on the composite permittivity and loss tangent (tan δ) values, as these dropped drastically by 60%. These materials are promising for the miniaturization of electronic components in microelectronics and telecommunications applications.

1. INTRODUCTION

Composite materials offer a strategic advantage in microwave applications due to properties unattainable by single materials alone [1, 2]. Through precise blending of constituents, composite materials with tailored properties can be achieved to meet specific performance requirements. Polymer-ceramic composites with high dielectric permittivity have seen widespread use in structural applications, particularly in mobile and satellite communication systems, antennas, oscillators, filters, capacitors, wireless communications, and sensors [3]. However, the direct experimental determination of complex dielectric permittivity in both solid and liquid states remains challenging.

In recent years, the advancement of microwave applications has been intricately linked to the dielectric properties of composite materials. The deployment of electromagnetic wave energy has expanded across various fields, including wireless communication, local area networks, and radar systems [4, 5].

Microwave-absorbing materials are employed in radiometer target calibration, electromagnetic shielding, and antenna design, necessitating a thorough characterization of frequency-dependent complex permittivity across wide frequency ranges. Accurate measurement and understanding of these dielectric properties are essential to comprehend microwave interactions with materials, as they influence both fundamental studies of composite structures and practical applications as wave absorbers. The dielectric relaxation behavior, dependent on the composite composition, provides crucial information on the relaxation processes and phase structures within these materials.

Various empirical theories and mixing laws are utilized to predict composite permittivity based on component measurements [6, 7]. The approach based on the modified Lichtenecker law (MLL) extends the application of shape factors to ternary mixtures, addressing limitations in traditional models. Our study further contributes to the field by examining the dielectric behavior of multiphase composites, comparing the effects of additives such as barium titanate ($BaTiO_3$) and silicon dioxide (SiO_2) to determine their influence on dielectric and electrical properties. Using the

MLL model with nonlinear optimization, this work corroborates experimental findings and offers insights into the design of materials suited for advanced microwave electronic applications [8, 9].

Owing to the importance of frequency dispersion in complex permittivity, understanding characterization techniques is necessary. Time Domain Spectroscopy (TDS) is particularly valuable due to its broad frequency coverage [10], positioning dielectric spectroscopy as a robust tool for investigating solid and liquid materials at multiple scales. In this work [10], experimental data are compared with theoretical predictions from proposed empirical models to assess the complex permittivity of resonance-type composites. The TDS technique, known for its extensive frequency range and analytical capabilities, has therefore emerged as a key method for investigating dielectric properties across diverse applications in industry, medicine, and agriculture.

The absorption characteristics of a material are determined by its complex permittivity and permeability: the real parts represent the material's ability to store electromagnetic energy, whereas the imaginary parts correspond to energy dissipation or loss. Composite properties are influenced by the dielectric permittivity and magnetic permeability of the fillers, as well as the matrix's inherent loss characteristics.

In this investigation, epoxy resin (RE) composites incorporating $BaTiO_3$ along with SiO_2 are characterized using TDS within the frequency range of DC–30 GHz. This allows for the evaluation of their dielectric permittivity. The modified Lichtenecker law, having demonstrated its efficiency in prior research work [11] and being enhanced by nonlinear regression optimization, is employed to model dielectric and magnetic behavior while accounting for the impact of grain morphology on composite properties.

This article investigates the influence of silica and $BaTiO_3$ on the dielectric behavior of ternary composites made of RE. Our study utilizes TDS data to model frequency-dependent behavior up. Moreover, it involves a simultaneous analysis aiming to determine the frequency limit up to which the composite provides a constant dielectric permittivity with a low dielectric loss factor. These dielectric parameters (ε' and ε'') provide valuable insights into the energy storage and dissipation characteristics of composites, which are essential for advanced applications in antenna design and other electronic components.

In addition, the exploration of multiphase composites over a broad frequency range reveals resonance effects, which are investigated in the presence of SiO_2 to assess its impact on the dielectric properties compared to other oxide inclusions [12].

These findings hold promise for future applications in electronic devices, including positive temperature coefficient (PTC) devices, pulse generators, infrared detectors, tunable microwave devices, multilayer ceramic capacitors, actuators, lead-free piezoelectric transducers, and charge storage devices.

Dielectric materials with enhanced permittivity and low dielectric loss are crucial for microwave electronics. Innovative requirements for miniaturization and cost reduction drive the development of high-performance materials. In some dielectrics, high permittivity with low loss has significant technical utility in high-frequency devices [13]. Dielectric oxide ceramics have transformed the microwave wireless communications industry by reducing size and cost for filters, oscillators, and antennas, fulfilling low-loss and permittivity requirements in devices such as satellite communication systems.

The outcomes of these research areas [14, 15] contribute to the development of materials that can miniaturize and optimize microwave microelectronic devices for telecommunications, including antennas, resonators, filters, and wave absorbers.

2. THEORETICAL FOUNDATIONS

2.1 Static dielectric study of composite

In this section, the permittivity is shown to be independent of frequency, but rather strongly related to the inclusion quantities. This state of dependence is effectively modeled by mixing laws, which approximately predict the dielectric behavior of these composites.

Several mixing laws have been used to describe the characteristics of a heterogeneous dielectric medium, such as the Wakino [7] and Maxwell-Garnett laws [16]. These models confirm that most of these laws are valid only for specific domains and certain types of composites. However, they do not yield accurate results for composites with grains of varying geometric shapes [17]. Another alternative, based on the Lichtenecker law, suggests a solution to the problems of mixture behavior; it is called the Modified Lichtenecker Law (MLL).

The MLL provides answers to the problem of material behavior in both binary and ternary compositions. Furthermore, it evaluates the dielectric permittivity and extends the complex permittivity modeling to the high-frequency range, reaching up to several GHz. The effective dielectric constant of the mixture is determined from the following relationship:

$$ln(\varepsilon_{\text{eff}}) = p_1\, ln\, \varepsilon_1 + p_2\, ln\, \varepsilon_2 \qquad p_1 + p_2 = 1 \tag{1}$$

The Modified Lichtenecker Law adds a new parameter A_l, it represents a shape factor in this equation:

$$\varepsilon_{eff} = A_l . \prod_{n=1}^{N} \varepsilon_n^{\alpha_n} \qquad with \quad \sum_{n=1}^{N} \alpha_n = 1 \tag{2}$$

For binary composite, the equation will be as follows:

$$\varepsilon_{eff} = A_l . \varepsilon_{C1}^{x} . \varepsilon_{C2}^{y} \tag{3}$$

$\varepsilon_{C1}^{x}, \varepsilon_{C2}^{y}$ are the dielectric constants of the mixture constituents**;** *x* and *y* are their respective volume fractions. For a ternary mixture, a third component dielectric parameter, $\varepsilon^{z}{}_{c3}$ must be added.

The Wiener limits are fundamental theoretical bounds used to estimate the effective dielectric constant of a composite material. They provide the upper and lower limits for the effective property based on the volume fractions and properties of the individual components. The equations are given as follows:

$$\frac{1}{\varepsilon_{lower}} = \frac{f}{\varepsilon_i} + \frac{(1-f)}{\varepsilon_m} \tag{4}$$

$$\varepsilon_{upper} = f . \varepsilon_i + (1-f) . \varepsilon_m \tag{5}$$

2.2 Dynamic dielectric study of composite

This theoretical analysis focuses on identifying the relaxation and resonance phenomena that the dielectric composite can exhibit across a wide frequency dispersion spectrum. This is made possible by the practical results revealed by the TDS measurement bench for the complex permittivity over a frequency range of up to 30 GHz.

In general, the examination of the dielectric parameters of a composite is carried out over this frequency band in order to observe the presence of relaxation and resonance phenomena. The mixing laws discussed in the previous section are only suitable for the quasi-static effective permittivity in this frequency range. This has led us to resort to the use of wide-band frequency dispersion models of complex permittivity, describing a dielectric behavior that can account for the above-mentioned phenomena.

To model this complex permittivity, numerical methods are used; they provide a predictive and accurate behavioral model of both relaxation and resonance phenomena. The Debye model, widely regarded as a foundational modeling approach from which others are derived; thus, the complex dielectric constant is given as:

$$\varepsilon^*(\omega) = \varepsilon_\infty + \frac{\varepsilon_s - \varepsilon_\infty}{1 + j\omega\tau} - j\frac{\sigma_s}{\omega\varepsilon_0} \tag{6}$$

where, σ_s is the static conductivity, τ is the relaxation time, ε_0 represents the vacuum permittivity, while $\varepsilon_s, \varepsilon_\infty$ denote the static (low-frequency) and high-frequency limit permittivity, respectively.

At a condition of $\varepsilon_s = \varepsilon_\infty$ and low frequency the imaginary part of dielectric permittivity will be as follows:

$$\varepsilon'' = \frac{\sigma_s}{\omega.\varepsilon_0} \tag{7}$$

Numerous frequency-domain models that provide an insightful description of the resonance effects. The scope of this work is confined to the most recent modeling approaches, as highlighted in this work [18]. One of the most effective models for describing this resonance behavior is the Lorentz model, whose equation is:

$$\varepsilon^* = \varepsilon_\infty + \frac{\varepsilon_s - \varepsilon_\infty}{1 + j\gamma\frac{f}{f_r} - \left(\frac{f}{f_r}\right)^2} \tag{8}$$

A derivative of this approach, known as the Choi model [19], introduces specific modifications to enhance the prediction of frequency-dispersive resonance behavior. The equation, deduced from the previous one is:

$$\varepsilon^* = \varepsilon_\infty + \frac{\varepsilon_s - \varepsilon_\infty}{\left(1 + j\gamma\frac{f}{f_r} - \left(\frac{f}{f_r}\right)^2\right)^\beta} \tag{9}$$

The proposed model for this study is inspired by Choi's modified model, incorporating a more optimal choice of the damping factor in order to align the experimental and theoretical results more closely. A comparison of the resulting data shows that the proposed model, when applied to ternary combinations, led to high accuracy [18].

3. PROTOCOL OF USE

3.1 The experimental procedure

The method used to measure the dielectric permittivity of the samples is Time Domain Reflectometry (TDR) as shown in Figure 1, which is based on the multiple reflection technique.

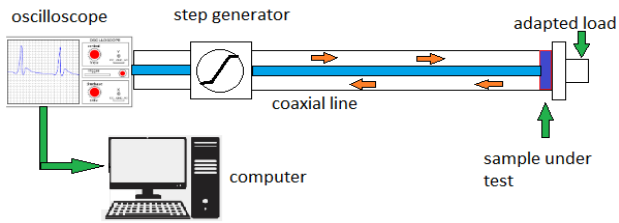

Figure 1. Time domain spectroscopy measurement

The experimental bench used for this measuring technique is set up using a step generator (HP54121 model) producing a 200 mV amplitude level with a rise time of 35 ps, a signal sampling head, and an oscilloscope mainframe (HP4120B model).

The step generator signal propagates along an APC-7mm precision-type standard coaxial guide with a characteristic impedance equal to 50 Ω. This line ends with a sample holder and a matched load to eliminate unwanted reflections.

The measurements are carried out over a wide frequency range of up to 30 GHz. The ratio of the reflected signal $V^-(\omega)$ to the incident signal $V^+(\omega)$ yields the reflection coefficient $\Gamma^*(\omega)$, which is the first variable to be calculated by applying a Fourier transform to the experimental data as follows:

$$\Gamma^*(\omega) = \frac{V^-(\omega)}{V^+(\omega)} \tag{10}$$

Another important parameter to be determined is the complex dielectric permittivity, which describes the dielectric and conductive aspects of the mixture through its real and imaginary parts. This is calculated from the admittance ratio and is expressed as follows:

$$\frac{Y_{in}}{Y_0} = \frac{\sqrt{\varepsilon^*}.tanh(s) + 1}{1 + j\frac{\omega_d\, tanh(s)}{c.s}} \tag{11}$$

where, Y_{in}, Y_0 are respectively the input admittance and the characteristic admittance; the value of S is represented by this relation:

$$s = j\frac{\omega_d}{c}.\sqrt{\varepsilon} \tag{12}$$

where, ω is the angular frequency, d is the thickness of the sample and c is the light speed in the vacuum. In order to solve this equation in the complex plane, numerical methods are employed, and many solutions can be found. The Debye model is considered to be one of the most effective, as discussed previously in the theoretical section.

3.2 Preparing samples

A series of samples were prepared for this study, including

both binary and ternary composite types. The materials used to synthesize these composites were $BaTiO_3$ and SiO_2. The first component, a perovskite structure, was chosen for its very high dielectric constant and low dielectric loss. These characteristics are highly valued in telecommunications systems and microelectronics. This material is used in the form of a white powder with a purity of 99%.

The second material, SiO_2, is a fine white powder with the same high purity as the first; however, it has a very low dielectric permittivity. As a robust insulator, it is highly valued in microelectronics, particularly in the manufacture of CMOS components. The addition of these components aims to tailor the dielectric properties; the composites are produced by immersing the fillers in a resin (RE) that acts as a binder, ensuring the adhesion of the particles.

RE was employed as the matrix in all samples to incorporate the various constituents. The volume fraction of the ternary mixture, as suggested in recent research [11], was distributed in a complementary manner between the resin and the fillers.

To avoid the viscosity problems faced in most previous research [11, 18, 20], the volume of RE was fixed at 70% during the mixing process. The two other loading elements of the mixture, $BaTiO_3$ and SiO_2, share the remaining 30% of the volume, with each varying from 0% to 30% in steps of 2.5%. It is important to clarify that the results obtained are related to this specific composition window.

On the other hand, two binary composites were prepared. The first is composed of RE, with a volume fraction varying from 100% to 55%, mixed with $BaTiO_3$ varying from 0% to 45% in steps of 5%. This same compositional range was applied to the second binary mixture based on RE and SiO_2. After hardening, the samples were machined to a toroidal shape to fit the size of the coaxial cell; measurements were made at room temperature and atmospheric pressure.

4. RESULTS AND DISCUSSION

4.1 Study of the dielectric behavior of RE-$BaTiO_3$ composites

It is observed that the effective permittivity values of this binary composite are almost constant over a frequency spectrum up to 10 GHz for all $BaTiO_3$ concentrations, as shown in Figure 2.

The theoretical curve was calculated using the Lichtenecker law and then compared to the experimental curve. A good agreement is achieved between them for low $BaTiO_3$ concentrations; however, the two curves start to diverge rapidly at higher concentrations. This indicates that the traditional Lichtenecker law approach does not adequately model high filler concentrations, as it assumes that the filler particles have identical shapes, whereas they are actually asymmetric and randomly oriented.

Consequently, recent research [11, 18] has suggested using a new approach, the MLL, which incorporates a shape factor A_l. The value of this shape factor can be calculated as follows:

$$A_l = \frac{\varepsilon_{eff}}{\varepsilon_{Re}^{x} . \varepsilon_{Tba}^{y}} \qquad (13)$$

where, $\varepsilon_{Re}^{x}, \varepsilon_{Tba}^{y}$ are the permittivity of resin and $BaTiO_3$ respectively, and x, y are the volume fractions of these two composite constituents.

Different approximations were evaluated in this new approach: linear, constant, and polynomial. The polynomial approximation provided the best fit for the experimental data; as a result, the MLL model is demonstrated to be valid for predicting the dielectric behavior of the RE-$BaTiO_3$ binary composite.

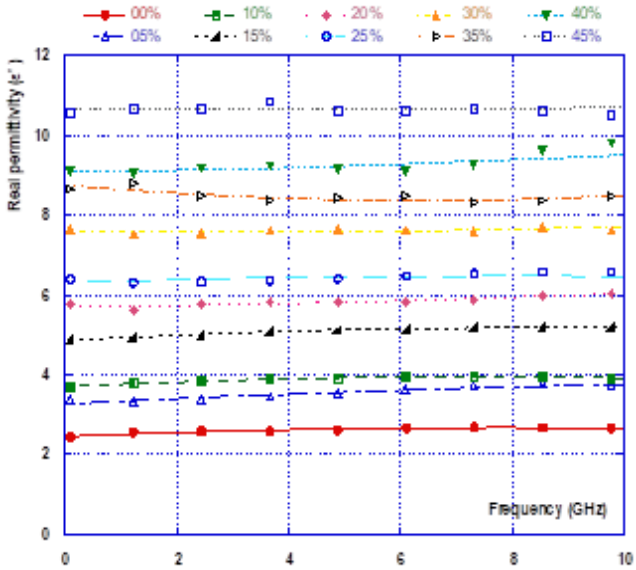

Figure 2. Frequency dependence of (ε′) for RE-$BaTiO_3$ binary composites

4.2 Study of the dielectric behavior of RE-SiO_2 composites

For this binary composite consisting of SiO_2 mixed with RE, Figure 3 displays the experimental and theoretical curves. The effective permittivity increases from 2.4 to 2.96 with increasing SiO_2 concentration. The theoretical real permittivity curve was calculated using the Modified Lichtenecker Law (MLL) approach.

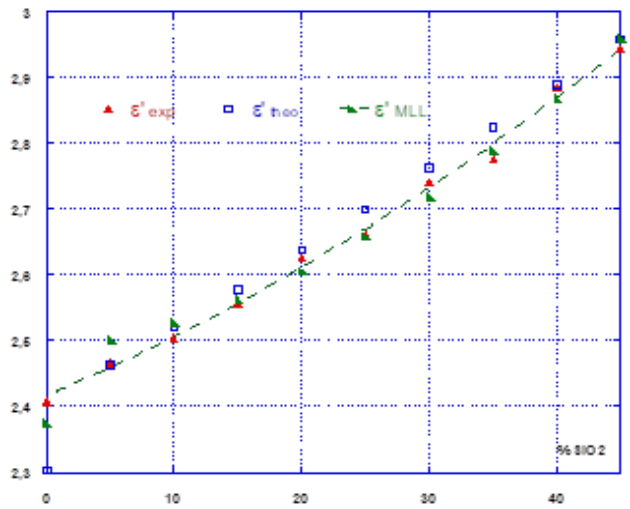

Figure 3. The real permittivity of RE-SiO_2 as a function of SiO_2 concentration

The model obtained shows good concordance with the experimental results, as demonstrated by the inclusion of the Wiener limits in Figure 4.

The MLL curve lies between the upper and lower bounds of the Wiener limits; thus, the MLL model again accurately

predicts the dielectric behavior of our binary composite.

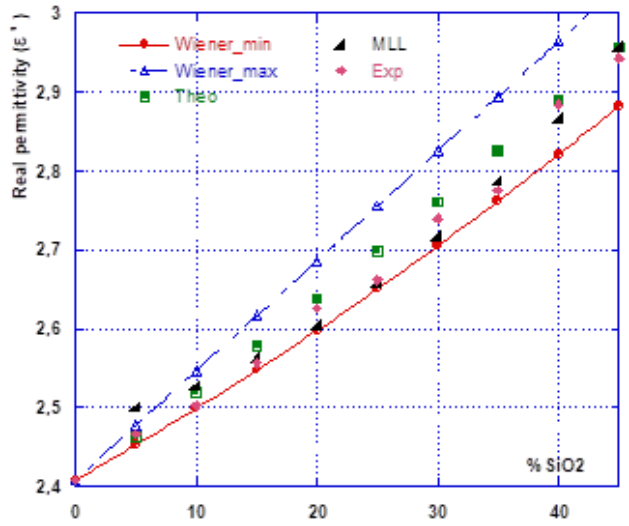

Figure 4. Comparing experimental and MLL model results with Wiener limits for RE-SiO_2 binary composite

4.3 Study of the dielectric behavior of RE-$BaTiO_3$-SiO_2 composites

This composite is composed of $BaTiO_3$, SiO_2, and RE, which is used as a matrix to bind the two elements together. The volume fraction of the RE was fixed at 70%. The remaining 30% of the mixture is complementarily divided between SiO_2 and $BaTiO_3$, with each varying in steps of 2.5%. This yielded 12 samples; however, one sample (5%SiO_2-25%$BaTiO_3$-70%RE) failed during the machining phase. The remaining samples were sufficient for this dielectric study of the ternary composite. Figure 5 illustrates the real permittivity curve for our ternary composite.

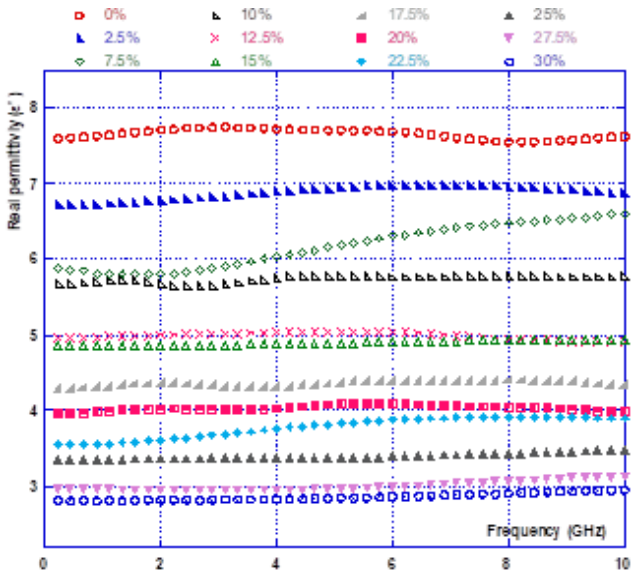

Figure 5. Frequency dependence of (ε′) for RE-$BaTiO_3$-SiO_2 ternary composites

The results show the variation of the permittivity as a function of SiO_2 concentration; the dielectric parameter value remains constant over a frequency range from DC to 10 GHz.

The experimental results for the permittivity of our ternary RE-$BaTiO_3$-SiO_2 composite are shown in Figure 6. While the theoretical curve was calculated using the Lichtenecker law, it is observed that this law does not provide precise results for this ternary system.

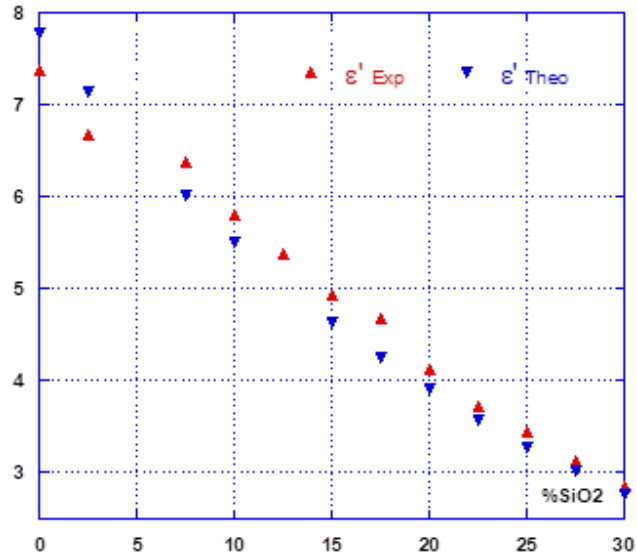

Figure 6. Experimental and theoretical permittivity of RE-$BaTiO_3$-SiO_2 composites as a function of SiO_2 content

For this reason, the MLL approach was introduced, and the shape factor A_l was calculated according to Eq. (13), as previously described. However, as this composite is a ternary system, the parameters for the third constituent must be incorporated, the equation will be as follows:

$$A_l = \frac{\varepsilon'_{eff}}{\varepsilon'^{x}_{Re} \cdot \varepsilon'^{y}_{TBa} \cdot \varepsilon'^{z}_{SiO2}} \tag{14}$$

The curve for A_l is presented in Figure 7. There are three methods to fit the curve to match the trend of the experimental data, namely: linear, constant value, and polynomial fitting.

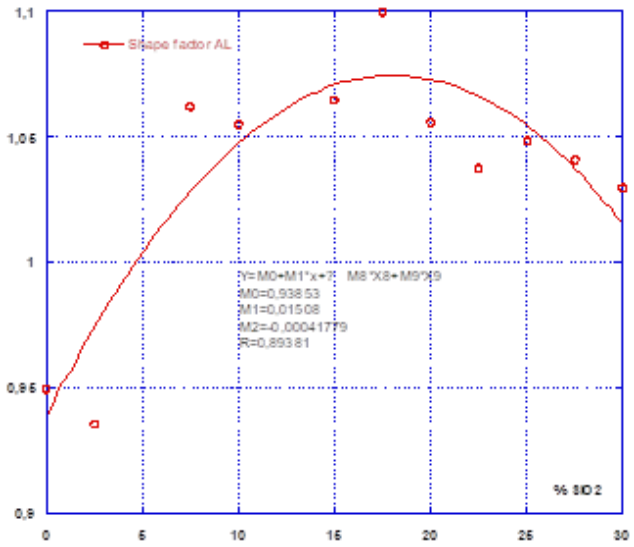

Figure 7. Shape factor for polynomial fitting

Considering the results obtained in prior work [11], the polynomial approach has proved to be the most convincing; therefore, it was chosen for the current work. The mathematical software used for this purpose allowed us to

determine the polynomial coefficients M0, M1 and M2 to ensure optimal smoothing. The effective permittivity of the ternary composite was then calculated using the MLL, and the resulting curve was plotted.

Figure 8 shows the experimental curve compared to both theoretical models: the basic Lichtenecker law and the Modified Lichtenecker Law (MLL).

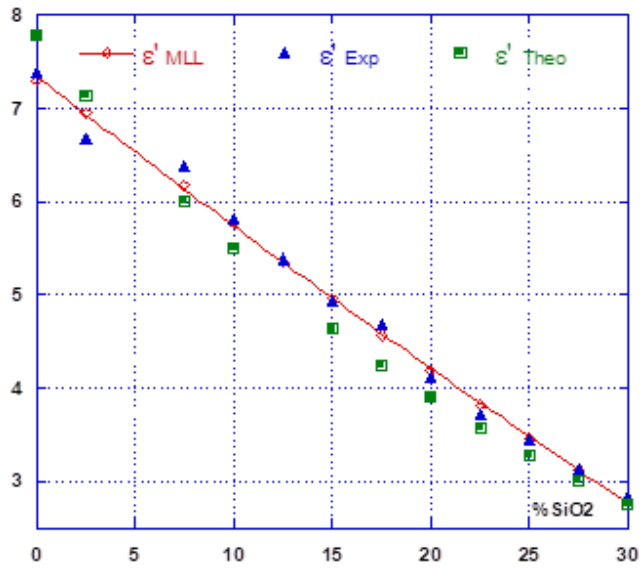

Figure 8. MLL model predictions against the experimental and theoretical results

The MLL has yielded superior results compared to the simple Lichtenecker law, confirming the same conclusion reached for binary composites. The MLL approach accurately predicts the behavior of both binary and ternary composites; moreover, its validity is confirmed by its location between the upper and lower Wiener bounds, as depicted in Figure 9.

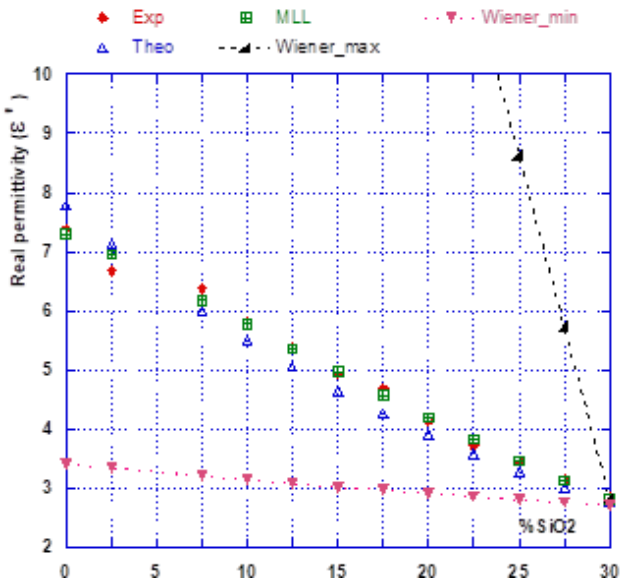

Figure 9. Validation of MLL model results against Wiener theoretical bounds

Calculating the real permittivity error using the optimization method provides insight into the accuracy of this model; this is achieved using the following equation:

$$Q = \left| \frac{\varepsilon'_{exp} - \varepsilon'_{the}}{\varepsilon'_{the}} \right| x\ 100 \qquad (15)$$

The error values in Table 1 range from approximately 1% to 2.5% and do not exceed 3% for any of the concentrations studied. Therefore, the modified Lichtenecker model remains highly relevant, providing a tolerable uncertainty margin for ternary composites [20].

Table 1. Statistical validation and accuracy of the MLL model for ternary composites

% SiO_2	0	2.5	7.5	10	12.5	15
Q	1.145	1.69	1.033	0.721	0.601	0.563
% SiO_2	17.5	20	22.5	25	27.5	30
Q	2.369	1.608	2.482	0.5457	0.346	1.488

4.4 modeling of broad-spectrum ternary composites

According to the exploration of dielectric behavior carried out over the specified frequency range, it was found that the real and imaginary permittivity for both types of composites are largely frequency-independent. Moreover, the predictive modeling based on the aforementioned mixing laws is conclusive regarding the influence of $BaTiO_3$ and SiO_2 inclusions.

On the other hand, the alteration of dielectric parameters as the working frequency exceeds the upper limits of the dispersion spectrum is characterized as a resonance phenomenon [18, 21]. One of the effective models for describing such resonance behavior is the Choi model, which was developed from the Lorentzian equation to achieve more precise results. Further modifications were made to the equation in a previous study [17], increasing the power of the frequency term $\left(f/f_r\right)$ from 2 to 4 to achieve better modeling of the resonance peaks in both the real and imaginary parts of the permittivity, the equation will be as follows:

$$\varepsilon^* = \varepsilon_\infty + \frac{\varepsilon_s - \varepsilon_\infty}{\left(1 + j\gamma\left(\frac{f}{f_r}\right)^2 - \left(\frac{f}{f_r}\right)^4\right)^\beta} \qquad (16)$$

It is suggested to introduce further modifications by increasing the power of the imaginary term $\left(f/f_r\right)$ from 2 to 4, and the power of the real term $\left(f/f_r\right)$ from 4 to 8, as presented in this equation:

$$\varepsilon^* = \varepsilon_\infty + \frac{\varepsilon_s - \varepsilon_\infty}{\left(1 + j\gamma\left(\frac{f}{f_r}\right)^4 - \left(\frac{f}{f_r}\right)^8\right)^\beta} \qquad (17)$$

A concentration of 10% SiO_2 has been taken as an example; the curves for the experimental complex permittivity and the Lorentzian approach using Eq. (16) and Eq. (17) are shown in Figure 10.

This work aims to determine the factor (β) by solving the equations mentioned above. To evaluate the accuracy of our proposed model, we compared it with experimental results

using an approximate mathematical optimization algorithm based on the FminSearch function implemented in MATLAB. The results of the proposed model are convincing, as Eq. (17) provides a superior fit compared to Eq. (16), particularly for the imaginary part of the effective permittivity, aligning more closely with the experimental values. Specific concentrations were selected as study examples to calculate the value of (β), as shown in Table 2.

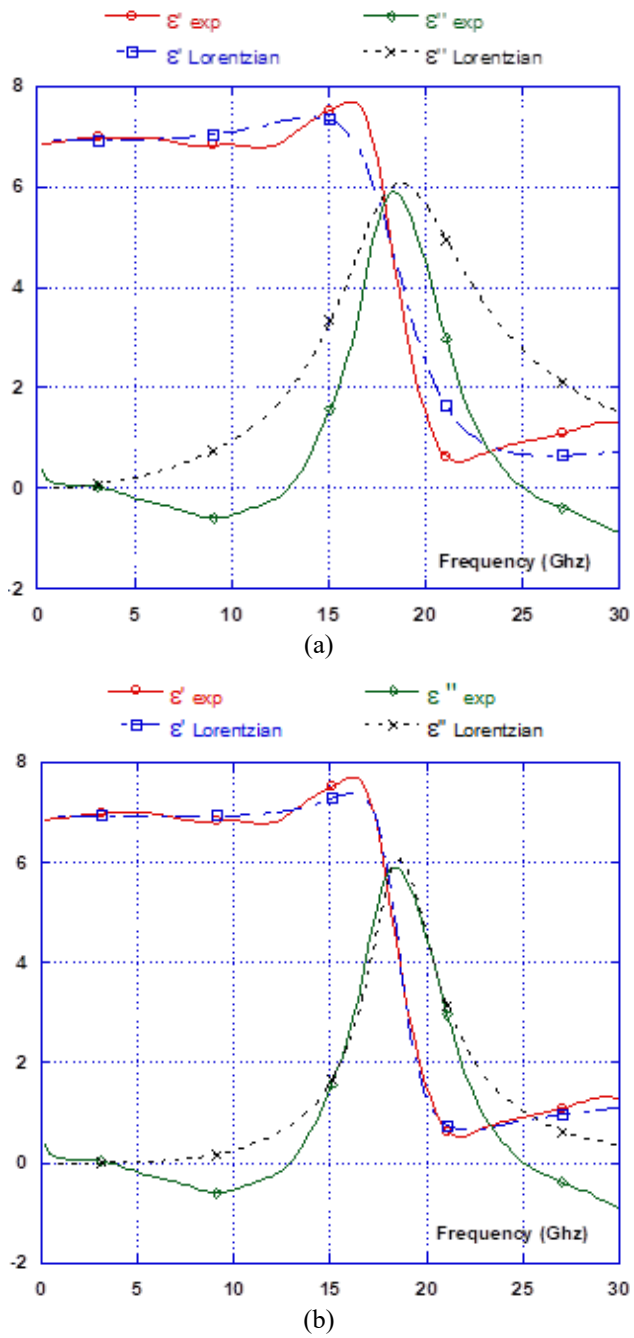

Figure 10. Experimental dielectric data and corresponding Lorentzian model fitting (a) Calculation from Eq. (16) (b) Calculation from Eq. (17)

Table 2. Evaluation of the factor β

SiO_2%	β (eq 16)	β (eq 17)
0	0.6729	0.6615
2.5	0.6828	0.6321
7.5	0.5808	0.555
22.5	0.6225	0.5743

4.5 Effect of SiO_2 on the dielectric RE-$BaTiO_3$ composites

The objective of this part of this section is to establish a way to analyze the effect of the SiO_2 on the dielectric of RE-$BaTiO_3$ binary composite across a wide frequency spectrum.

4.5.1 Frequency domain analysis

The experimental values for the real effective permittivity of the RE-$BaTiO_3$-SiO_2, RE-SiO_2 and RE-$BaTiO_3$ composites were recorded. The influence of the inclusion volume fraction on the permittivity is quantifiable. A comprehensive analysis of the collected data yields the following observations:

The data provided by the RE-SiO_2 composite shows minimal variation in the real permittivity of the binary mixture, despite the gradual inclusion of SiO_2 concentrations. The recorded difference in ε' is approximately 0.56 between the minimum and maximum volume fractions. This is explained by the oxide dielectric behavior of the $\varepsilon' = 3{,}8$ being relatively close to that of the resin $\varepsilon' = 2{,}4$; consequently, this binary composite exhibits limited tunability in terms of dielectric permittivity.

Conversely, this binary composite allows for a significant shift in real dielectric permittivity, increasing from 2.40 to 10.84. This evolution is attributed to the high permittivity of $BaTiO_3$ (ε'=120) compared to the RE matrix. This highlights the substantial impact that high-permittivity fillers have on the overall mixture.

For the ternary RE-$BaTiO_3$-SiO_2 composite, the resin content was maintained at 70%. The dielectric behavior shows a clear improvement in permittivity, ranging from 2.84 to 7.38 (a difference of 4.54). This change occurs as $BaTiO_3$ is incrementally replaced by SiO_2. Consequently, it can be concluded that incorporating SiO_2 into the RE-$BaTiO_3$ composite effectively reduces the overall real permittivity ε'.

4.5.2 Time domain analysis

The variation in the pulse peak and width is directly related to the permittivity values. For the RE-$BaTiO_3$ binary composite in Figure 11, as $BaTiO_3$ content increases, the normalized voltage dip becomes deeper and wider. This indicates a stronger and more prolonged interaction of the pulse with the high-permittivity composite.

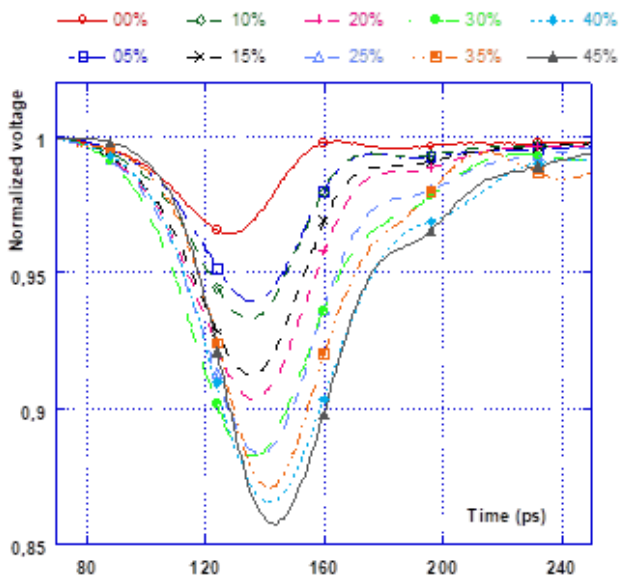

Figure 11. Normalized voltage of RE-$BaTiO_3$ composites as a function of $BaTiO_3$ in temporal domain

The RE-$BaTiO_3$-SiO_2 ternary composite further confirms this observation in Figure 12. A 0% SiO_2 concentration (representing 30% $BaTiO_3$) results in high permittivity. As $BaTiO_3$ is replaced by SiO_2, the permittivity decreases, causing the reflected pulse to become faster and weaker; thus, the normalized voltage dip becomes shallower and narrower.

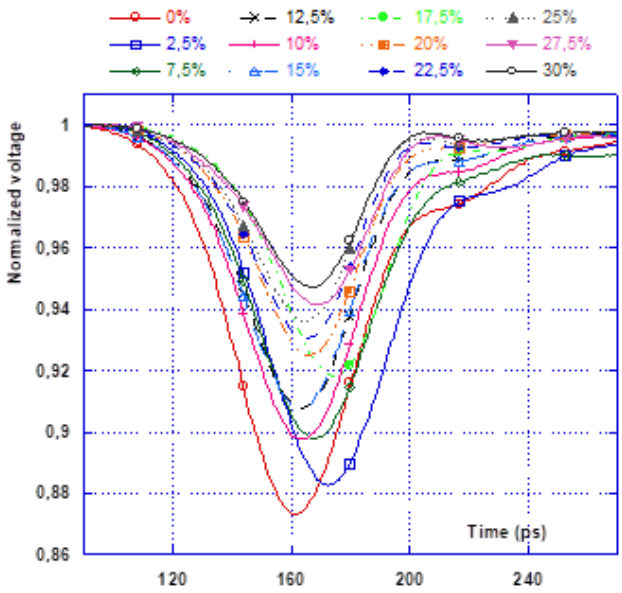

Figure 12. Normalized voltage of RE-$BaTiO_3$-SiO_2 composites as a function of SiO_2 in temporal domain

The physical interpretation of these results is as follows: a higher permittivity indicates that the material can store more electrical energy. This increased energy storage results in slower pulse propagation through the material because the electric field interacts more intensely with the dielectric medium.

As the pulse slows down in a dispersive medium, it spreads out; this temporal broadening reduces the peak amplitude because the pulse energy is distributed over a longer duration. In summary, analyzing the width and shape of the reflected pulse provides valuable quantitative information regarding the material's permittivity

4.5.3 Analysis of dissipated energy

Another parameter is the loss tangent (tan δ), which is used to highlight changes in the dielectric properties of a mixture or to compare differences between mixtures. Also known as the dissipation factor, it characterizes the amount of electromagnetic energy transformed into heat within the material. It is defined as the ratio of the imaginary part $\varepsilon''(w)$ to the real part $\varepsilon'(w)$ of the permittivity at a given frequency, expressed as follows:

$$\delta(w) = \frac{\varepsilon''(w)}{\varepsilon'(w)} \qquad (18)$$

A high loss tangent indicates that the material has significant dielectric absorption and substantial power loss during transmission. For instance, the radiation efficiency of an antenna is inversely related to the loss factor; a large loss tangent results in significantly reduced radiation efficiency.

The objective of this analysis is to determine the role of SiO_2 in improving this parameter. Table 3 presents the values of tan δ as a function of real permittivity for both binary and ternary composites. The permittivity values were recorded at 450 MHz, a frequency selected due to the observed stability of the imaginary permittivity in this range. Previous study [22] has noted instabilities at frequencies above 1 GHz; therefore, 450 MHz was identified as the optimal frequency for ensuring consistent and reliable measurements.

Table 3. Dielectric loss (tan δ) as a function of ε' for RE-$BaTiO_3$-SiO_2 mixtures

RE-$BaTiO_3$		RE-$BaTiO_3$-SiO_2	
ε'	$tan\ \delta\ (\varepsilon''/\varepsilon')$	ε'	$tan\ \delta\ (\varepsilon''/\varepsilon')$
7.4826	0.1686	7.384	0.073
5.8376	0.1893	5.811	0.056
3.3367	0.2433	3.441	0.0986

In this comparison, a binary $BaTiO_3$ composite is evaluated against a ternary composite incorporating SiO_2. By selecting samples with real permittivity values in the same range (3 to 7), a direct comparison is possible:

For a permittivity $\varepsilon' = 3.3367$ in the RE-$BaTiO_3$ binary composite, the loss tangent is $\delta = 0.2433$.

The closest ternary RE-$BaTiO_3$-SiO_2 sample ($\varepsilon' = 3.441$) exhibits a loss tangent tan $\delta = 0.0986$. In this case, the dissipated energy in the binary composite is more than twice that of the ternary composite. A similar trend is observed for permittivity values (ε') near 5.8 and 7.3.

In electronic applications, high dielectric losses convert electrical energy into heat, which can damage sensitive components, reduce device lifespan, and necessitate complex cooling mechanisms. Consequently, combining SiO_2 with $BaTiO_3$ effectively reduces dielectric loss, offering a distinct advantage for its use as a practical dielectric composite in modern electronic devices.

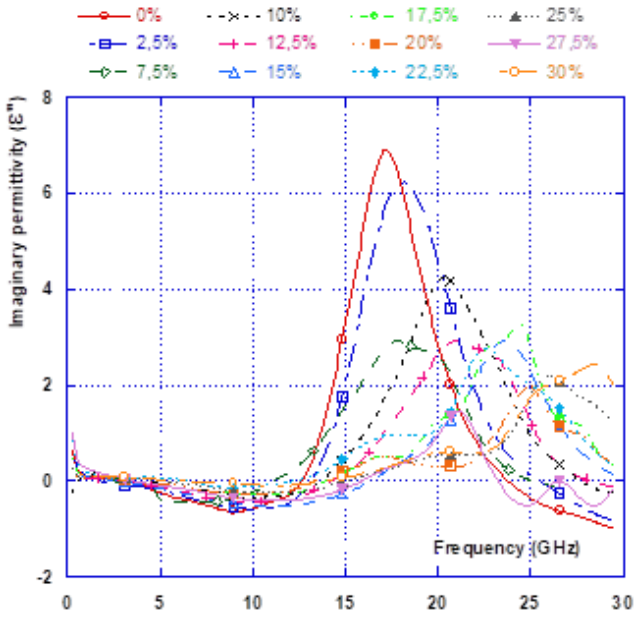

Figure 13. Comparison of resonance frequencies across various concentrations of the RE-$BaTiO_3$-SiO_2 composites

4.5.4 Dielectric relaxation and resonance phenomena

This part of the study focuses on two fundamental phenomena: relaxation and resonance. The imaginary part of the permittivity (ε'') is directly related to the resonance

frequency of the composite material. At these resonant frequencies, the material's response is dominated by energy dissipation mechanisms, causing ε″ to increase significantly. This frequency region corresponds to the maximum absorption of electromagnetic waves and the highest dielectric losses. As illustrated in Figure 13, the RE-$BaTiO_3$-SiO_2 ternary composite served as the central subject of this investigation.

It is observed that the ε″ values remain constant, near zero, for all concentrations at frequencies up to 10 GHz. However, from 10 GHz to 30 GHz, a distinct change in the curve profile occurs: it rises sharply to reach a maximum peak before falling abruptly to its lowest level. For each specific concentration, the curve begins to ascend at a unique point, identified as the resonance frequency (f_r).

Similarly, the real part of the permittivity (ε′) remains constant for all concentrations of the constituents (SiO_2 in this case) up to 10 GHz. As the frequency increases further, the curve exhibits a slight rise followed by a considerable drop to a minimum value. For each concentration, this reduction in value occurs at a distinct frequency, as shown in Figure 14, it is known as the relaxation frequency.

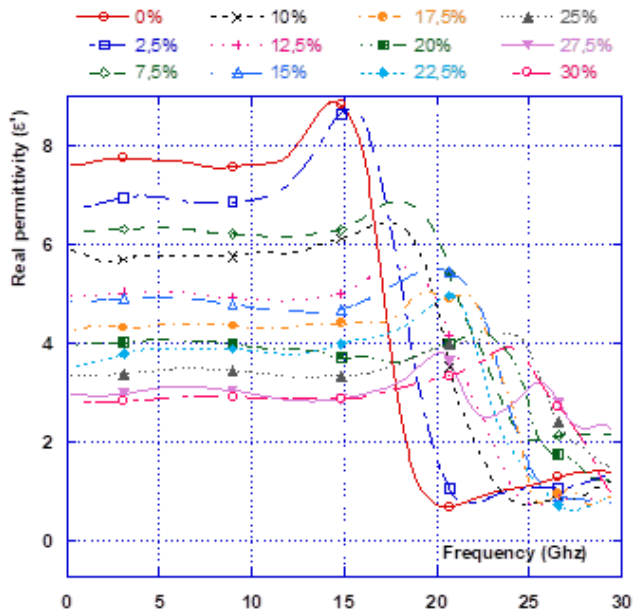

Figure 14. Dielectric relaxation behavior of RE-$BaTiO_3$-SiO_2 ternary composite at various filler concentrations

Resonance frequency refers to the frequency at which a system or material exhibits maximum response to an external driving force. In the context of dielectric materials, this often involves the frequency at which the material's response to an electric field is the strongest, leading to significant absorption or reflection of electromagnetic waves.

The relaxation frequency is the point at which the material's dielectric response transitions due to its internal polarization mechanisms. It is associated with the relaxation time required for dipoles or other polarizable entities to realign in response to an alternating electric field. Below the relaxation frequency, the material primarily stores energy. Above this frequency, dissipation mechanisms become dominant, leading to an increase in ε″. The relaxation frequency serves as the critical transition point between these two regimes.

In the RE-$BaTiO_3$-SiO_2 ternary composite, the highest permittivity (ε'_{eff} =7.38) occurs in the absence of SiO_2. This high permittivity corresponds to a slower relaxation time, shifting the relaxation frequency to a lower value (16 GHz). Because high-permittivity materials are capable of storing more energy, the peak of the imaginary part of the permittivity is at its maximum in this state.

Conversely, the inclusion of SiO_2 reduces the dielectric nature of the composite, decreasing the real permittivity to (ε'_{eff} =2.84). This reduction generally results in an increase in the resonance frequency, reaching approximately 25 GHz. A lower permittivity implies reduced energy storage, which alters the material's interaction with the electromagnetic field and shifts the resonance toward higher frequency values.

In conclusion, the addition of SiO_2 to the binary composite has a measurable impact on the resonance frequency, causing it to shift upward. This enhancement provides a significant advantage for the ternary composite, making it highly suitable for high-frequency applications where improved efficiency and broader bandwidth are required.

5. CONCLUSIONS

In this paper, heterogeneous binary and ternary composites (comprising RE-SiO_2, RE-$BaTiO_3$ and RE-SiO_2-$BaTiO_3$) were investigated to characterize their dielectric properties and evaluate the enhancements provided by each filler (SiO_2 and $BaTiO_3$). The analysis focused on the influence of inclusion concentrations and a wide frequency spectrum ranging from DC to 30 GHz.

The experimental results indicated that while the RE-SiO_2 binary composite reached a maximum permittivity of only 2.94, the RE-$BaTiO_3$ binary composite exhibited a significantly higher effective permittivity, peaking at 10.84. The transition to the RE-SiO_2-$BaTiO_3$ ternary system yielded compelling dielectric characteristics. Although the maximum permittivity decreased to 7.38 compared to the RE-$BaTiO_3$ binary system, the ternary composite achieved a vastly superior loss tangent (tan δ). For instance, at a matched permittivity of approximately 3.44, the loss tangent dropped from 0.24 in the binary system to 0.098 in the ternary system. This confirms that SiO_2 inclusion significantly minimizes energy dissipation, offering a critical advantage for high-efficiency electronic devices.

The MLL approach proved to be a highly effective tool for predicting the dielectric behavior of both binary and ternary mixtures. By modeling the grain shape factor as a second-order polynomial, a superior fit between theoretical and experimental data was achieved, a validation further supported by the Wiener limit bounds.

Furthermore, our study established that the relaxation and resonance frequencies are inherently linked to the composite's permittivity. Higher permittivity in the mixture results in a slower relaxation time and increased energy storage, which shifts the resonance frequency toward the lower end of the spectrum (16 GHz). Conversely, increasing the volume fraction of SiO_2 reduces the permittivity and shifts the resonance toward higher frequencies.

Finally, the Lorentz and Choi models were successfully utilized to establish the relationship between resonance frequency and the SiO_2 volume fraction. The empirical modifications described in this work proved essential for accurately modeling the dispersive behavior of ternary composites. Optimization using MATLAB algorithms yielded theoretical curves that align closely with experimental

observations, confirming the robustness of the proposed modeling framework.

REFERENCES

[1] Martinez-Vega, J. (2013). Dielectric Materials for Electrical Engineering. John Wiley & Sons.

[2] Nelson, J.K. (2010). Dielectric Polymer Nanocomposites (Vol. 226). Springer, New York, NY, USA.

[3] Dinda, P.T., Pierre, M. (2017). Electromagnétisme - Ondes et propagation guidée: Ondes et propagation guidée. https://www.abebooks.fr/Electromagn%C3%A9tisme-Ondes-propagation-guid%C3%A9e-Tchofo-Dinda/22543408034/bd.

[4] Dupeux, M. (2004). Science des Matériaux. Paris, France: Dunod.

[5] Lévêque, L., Diaham, S., Valdez-Nava, Z., Laudebat, L., Thierry, L. (2015). Effects of filler content on dielectric properties of epoxy/$SrTiO_3$ and epoxy/$BaTiO_3$ composites. In 2015 IEEE Conference on Electrical Insulation and Dielectric Phenomena (CEIDP), Ann Arbor, MI, USA, pp. 701-704. https://doi.org/10.1109/CEIDP.2015.7352070

[6] Ezquerra, T.A., Nogales, A. (2020). Crystallization as Studied by Broadband Dielectric Spectroscopy. Springer International Publishing, Cham, Switzerland.

[7] Wakino, K., Okada, T., Yoshida, N., Tomono, K. (1993). A new equation for predicting the dielectric constant of a mixture. Journal of the American Ceramic Society. 76(10): 2588-2594. https://doi.org/10.1111/j.1151-2916.1993.tb03985.x

[8] Zha, J.W., Dang, Z.M. (2023). High Temperature Polymer Dielectrics: Fundamentals and Applications in Power Equipment. John Wiley & Sons.

[9] Ganguly. S., Margel. S., Das. P. (2024). Magnetic Polymer Composites and Their Emerging Applications. CRC Press.

[10] Martin, J.C., Forniés-Marquina, J.M., Bottreau, A.M. (2003). Application of permittivity mixture laws to carbon black dielectric characterization by time domain reflectometry. Molecular Physics, 101(12): 1789-1793. https://doi.org/10.1080/0026897021000018367

[11] Brahimi, A., Bourouba, N., Jiménez, J.P.M., Bouzit, N. (2021). A high frequency dielectric behavior modeling of a ReXTMnO2 ternary composite as an equivalent binary mixture. Revue des Composites et des Matériaux Avancés-Journal of Composite and Advanced Materials, 31(4): 181-191. https://doi.org/10.18280/rcma.310401

[12] Kudelcik, J., Jahoda, E., Kurimsky, J. (2019). The effect of SiO_2 nano-filler on dielectric properties of epoxy resin. The European Physical Journal Applied Physics, 85(1): 10401. https://doi.org/10.1051/epjap/2019180221

[13] Zhao, C., Huang, Y., Wu, J. (2020). Multifunctional barium titanate ceramics via chemical modification tuning phase structure. InfoMat, 2(6): 1163-1190. https://doi.org/10.1002/inf2.12147

[14] Lee, C.S., Martino, A., Cong, R. (2024). Applications of Carbon Nanomaterials and Silicon-based Hybrid Composites in Lithium-ion Batteries. Cambridge Scholars Publishing.

[15] Moharana, S., Badapanda, T., Satpathy, S.K., Mahaling, R.N., Kumar, R. (2023). Perovskite Metal Oxides: Synthesis, Properties, and Applications. Elsevier.

[16] Sihvola, A. (2000). Mixing rules with complex dielectric coefficients. Subsurface Sensing Technologies and Applications, 1: 393-415. http://doi.org/10.1023/A:1026511515005

[17] Hasan, N., Noordin, N. H., Karim, M.S.A., Rejab, M.R.M., Ma, Q.J. (2020). Dielectric properties of epoxy–barium titanate composite for 5 GHz microstrip antenna design. SN Applied Sciences, 2(1): 62. https://doi.org/10.1007/s42452-019-1801-9

[18] Khouni, H., Bouzit, N. (2020). Study of the relaxation and resonance behaviors of ternary composites: Epoxy–strontium titanate–carbon black. Polymers and Polymer Composites, 28(7): 451-461. https://doi.org/10.1177/0967391119887573

[19] Choi, H.D., Cho, K.Y., Han, S., Yoon, H.G., Moon, T.J. (1998). Frequency dispersion characteristics of the complex permittivity of the epoxy-carbon black composites. Journal of Applied Polymer Science, 67(2): 363-369. https://doi.org/10.1002/(SICI)1097-4628(19980110)67:2%3C363::AID-APP17%3E3.0.CO;2-Z

[20] Delfouf, R., Bouzit, N., Bourouba, N., Martinez Jimenez, J.P., Brahimi, A., Khouni, H., Arab, T. (2022). Dielectric characterization and modeling of composite materials based on epoxy resin/black iron oxide/titanates in several frequency ranges. ECS Journal of Solid State Science and Technology, 11(7): 073006. https://doi.org/10.1149/2162-8777/ac7f55

[21] Kazaoui, S., Ravez, J. (1993). Dielectric relaxation in $Ba(Ti_{0.8}Zr_{0.2})O_3$ ceramics prepared from sol-gel and solid state reaction powders. Journal of Materials Science, 28(5): 1211-1219. https://doi.org/10.1007/BF01191955

[22] Bouchaour, M., Jiménez, J.P.M., Bouzit, N., Bourouba, N. (2018). Dielectric behavior of a quaternary composite (RE, BT, MnO_2, CaO) in the band (DC–2 GHz). The European Physical Journal Applied Physics, 84(1): 10201. https://doi.org/10.1051/epjap/2018180056

NOMENCLATURE

C	Speed of light in the vacuum, m. s^{-1}
D	The sample thickness, m
Ω	The angular frequency, rad. s^{-1}

Greek symbols

ε	The permittivity, F. m^{-1}
σ	The conductivity, Ω^{-1}. m^{-1}
β	The relative error for a given composite
Q	The asymmetric factor
T	The relaxation time, s
$\Gamma*$	Reflexion coefecient
Y	The admittance, S
γ	The damping factor

Subscripts

Al	The shape factor from the MLL
εeff	The effective permittivity of a mixture
ε_∞	The high frequency permittivity
ε_0	The vacuum permittivity, F. m^{-1}
ε'	The real permittivity, F. m^{-1}

ε''	The imaginary permittivity, F. m^{-1}	σ_s	The static conductivity, Ω^{-1}. m^{-1}
ε'_{the}	The theoretical dielectric permittivity	Y_{in}	The input admittance, S
ε'_{Exp}	The experimental dielectric permittivity	Y_0	The characteristic admittance, S